npg

Anthraquinone-2-sulfonic acid (AQ2S) is A Novel Neurotherapeutic Agent

TC Jackson*,[1], JD Verrier[2] and PM Kochanek[1]

Anthraquinone derivatives such as emodin have recently been shown to protect in models of beta amyloid β (Aβ) and tau aggregation-induced cell death. The mechanisms of action possibly involve preconditioning effects, anti-aggregation properties, and/or enhancing the phosphatidylinositol-3-kinase (PI3K)/AKT survival mechanism. We studied several natural (emodin, rhein, and aloin) and synthetic (AQ2S) anthraquinones, to screen for post-treatment therapeutic benefit in two models of neuronal death, namely hydrogen peroxide (H_2O_2) and staurosporine (STS)-induced injury. Treatment with emodin, rhein, or aloin failed to reduce H_2O_2 injury. Moreover, consistent with emodin behaving like a mild toxin, it exacerbated oxidative injury at the highest concentration used (50 μM) in our post-treatment paradigm, and potently inhibited AKT. In contrast, AQ2S was neuroprotective. It reduced H_2O_2 injury at 50 and 75 μM. In addition, AQ2S potently inhibited staurosporine (STS)-induced injury. The mechanisms of action involve caspase inhibition and AKT activation. However, blockade of AKT signaling with LY294002 failed to abolish AQ2S-mediated protection on the STS assay. This is the first study to report that AQ2S is a new neuroprotective compound and a novel caspase inhibitor.

Quinones are a unique class of organic compound identified by the presence of a cyclic diketone structure. The simplest example is 1,4-benzequinone (BQ). BQ consists of a single benzene ring flanked by 2 ketone [R-C(=O)] groups at the first and fourth carbons. 9–10-anthraquinone (AQ) is slightly more complex. AQ is derived from the three-ring aromatic structure anthracene.

Anthraquinones constitute a large and diverse subgroup within the quinone superfamily. Anthraquinone-based drugs are used as chemotherapeutic agents[1,2] and laxatives.[3] Moreover they show promise as treatments for malaria,[4,5] and multiple sclerosis.[6,7]

Recent studies show that some natural anthraquinones are also neuroprotective. The compound 6-methyl-1,3,8-trihydroxyanthraquinone (emodin) is a promising therapeutic agent with possible indications for the treatment of neurodegenerative disease. It inhibits aggregation of pathological tau,[8] and prevents β-amyloid-induced neuronal death in vitro.[9] Moreover, pre-treatment with emodin prevents H_2O_2-induced death of cortical neurons.[10] Finally, in vivo administration of emodin-8-O-β-D-glucoside reduces infarct volume after focal cerebral ischemia in rodents. Superoxide dismutase (SOD)

activity was increased, and lipid peroxidation decreased, by the emodin analog in this study.[11]

The anti-aggregation activity of emodin may be a shared trait amongst anthraquinones. AQ intercalates with β-amyloid sheets, and efficiently prevents aggregation of toxic Aβ-$_{1-40}$.[12] Furthermore, Colombo et al.[13] found that the chemotherapeutic anthraquinones mitoxantrone and pixantrone prevent aggregation of toxic (soluble) Aβ-$_{1-42}$.[13] Pixantrone also inhibited Aβ-$_{1-42}$ toxicity in neuroblastoma cells.

Finally, 1,8-dihydroxyanthraquinone (danthron) prevents death of neuron/glia co-cultures in five models of oxidative injury. It reduces death by toxic Aβ, Fe^{3+} peroxidation, glutathione depletion, nitric oxide radicals, and H_2O_2. However, danthron was ineffective against zinc toxicity, O_2^- radicals, N-methyl-D-aspartic acid, kainate, staurosporine (STS), or dextromethorphan.[14]

The neuroprotective mechanism(s) induced by emodin are unclear. Addition of LY294002, a phosphatidylinositol-3-kinase/AKT inhibitor, blocked its pro-survival action in the Aβ toxicity assay.[9] This suggests that AKT has an important role in emodin-induced protection. However, Aβ robustly inhibits endogenous AKT activity in both primary neurons[15]

and cerebrovascular endothelial cells.[16] Thus, emodin (as an aggregate inhibitor) may simply relieve Aβ-induced AKT repression. Furthermore, arguing against a direct stimulatory effect of emodin on AKT activation, studies report that it is a potent PI3K inhibitor (IC$_{50}$ 3.3 μM).[17,18] Moreover, studies in cancer cells report that emodin stimulates oxidative injury and promotes cell death.[19,20] Thus, at non-lethal doses, it may induce a preconditioning response in neurons, and protect against subsequent injury.

We tested if post-treatment with emodin ameliorated neuronal injury after an oxidative insult. Moreover, to identify new AQ-based neuroprotectants, we tested if post-treatment with rhein, aloin, or AQ2S reduces oxidative injury. Only AQ2S protected neurons in our study. We focused our efforts on validating AQ2S as a novel therapeutic agent, and sought to elucidate the mechanisms involved in neuroprotection.

Results

Post-injury treatment with natural anthraquinones does not prevent H$_2$O$_2$-induced neuronal death. We first developed a sensitive H$_2$O$_2$ injury protocol (Supplementary Figure 1). Cortical neurons were harvested and grown in neurobasal media containing B27 in the presence of antioxidants for 3 days. Prior studies show that neurons do not require antioxidants to survive after the first 24 h.[21] Therefore, fresh neurobasal media was prepared without antioxidants (i.e., B27–AO) for subsequent media exchanges. At D.I.V. 10–11, maintenance media was replaced with unsupplemented neurobasal (i.e., without B27) containing H$_2$O$_2$ and incubated for 35 min. Neurons were returned to fresh neurobasal/B27 (–AO) media, and cell viability measured 24 h later. As expected, even low concentrations of H$_2$O$_2$ (25–50 μM) significantly increased TUNEL staining (Supplementary Figures 1A–E), significantly decreased cell viability (Supplementary Figure 1F), and increased caspase-3/7 activity (Supplementary Figures 1G and H). From these preliminary results, we extrapolated the optimal 40 μM H$_2$O$_2$ dose to screen neuroprotection of test compounds.

Insulin like growth factor-1 (IGF-1) stimulates IGF-1 receptor phosphorylation (Figure 1a-western blot insert), and is an established *in vitro* and *in vivo* neuroprotectant.[22,23] It is effective if administered before (pre-treatment), but not after H$_2$O$_2$ insult.[24–26] The mechanism(s) involve H$_2$O$_2$-mediated inactivation of neuronal IGF-1 receptor signaling.[27] Because H$_2$O$_2$ injury induces major derangements in cell signaling, and is an important component to many forms of acute brain injury, we sought to test if anthraquinones could prevent neuronal death when applied after H$_2$O$_2$ injury. To validate cell signaling derangement in our system, H$_2$O$_2$-injured neurons were subsequently treated with 100 ng/ml IGF-1. Post-treatment with IGF-1 failed to rescue neurons from H$_2$O$_2$ injury (Figures 1a-d). The natural anthraquinones rhein (Figure 1a) and aloin (Figure 1b) were also ineffective at any concentration tested 24-h post-injury. Unexpectedly, 5 and 25 μM emodin (Figure 1c) failed to protect neurons from H$_2$O$_2$. Moreover, 50 μM emodin exacerbated cell death. Alternatively, 50 μM AQ2S significantly reduced

H$_2$O$_2$-induced cell death (Figure 1d). To validate the results, we compared the worst and best anthraquinones (emodin *versus* AQ2S) on a caspase 3/7 activity assay. Compared with control injury, emodin significantly reduced caspase activity at all three concentrations (Figure 1e). Similarly, AQ2S inhibited caspase 3/7 activity at both the 25 and 50 μM concentrations, but not at the lowest 5 μM concentration (Figure 1f).

AQ2S was the only compound able to inhibit cell death when given after H$_2$O$_2$ injury. Thus we focused our efforts to validate AQ2S-mediated neuroprotection. The H$_2$O$_2$ injury assay was repeated using a higher concentration of AQ2S. 75 μM AQ2S potently prevented cell death induced by 40 μM H$_2$O$_2$, measured 24 h after injury (Figure 2a). Moreover, consistent with prior results, 75 μM AQ2S significantly inhibited caspase 3/7 activity below injured and non-injured levels (Figure 2b).

AQ2S prevents classic STS-induced cell death. STS is an established inducer of caspase-mediated apoptotic cell death in neurons.[28–30] To further authenticate AQ2S as a novel neuroprotective compound, we subjected cortical neurons to STS injury ± AQ2S. In preliminary dose–response experiments, we found that 150 nM STS for 24 h optimally decreased viability measured by a live-cell protease activity assay (Supplementary Figure 2A) and increased lactate dehydrogenase (LDH) release (Supplementary Figure 2B). Co-treatment with 75 μM AQ2S significantly reduced 24 h STS injury determined by four different assays: resazurin metabolism (CellTiter Blue; Figure 3a), LDH release (Figure 3b), cellular ATP levels (GLO-Viability Assay; Figure 3c), and live-cell protease activity (CellTiter-Fluor; Figure 3d). AQ2S alone did not significantly alter baseline viability or cytotoxicity.

48-h high-dose (500–1000 nM) STS induces caspase-independent cell death mechanisms in neurons.[31] We tested if AQ2S prevents neuronal death after 24-h incubation with 500 nM STS. This concentration of STS resulted in near total death of neurons. Co-treatment with AQ2S only slightly augmented neuronal viability at 125 and 150 μM (Supplementary Figure 3).

AQ2S is a novel caspase-3 inhibitor. Incubation of cortical neurons with 250 nM STS for 24 h significantly induced cell death (Supplementary Figure 4A; 81.1% decrease in neuronal viability), and robustly upregulated caspase3/7 activity (Supplementary Figure 4B).

STS injury was repeated in the absence or presence of AQ2S. Similar to prior results, 250 nM STS reduced viability by 71.5% after 24 h. Co-treatment with either 75 or 125 μM AQ2S significantly reduced cell death (Figure 4a). AQ2S-treated neurons showed a 17.6% reduction in viability, compared with non-injured controls, after 24 h STS. Moreover, AQ2S completely blocked STS-induced caspase-3 activation, and inhibited caspase-3 activity below baseline levels (Figure 4c). Both AQ2S and Emodin were evaluated on an *in vitro* caspase-3 inhibitor drug screening assay. Only AQ2S and ZVAD-fmk significantly reduced the activity of recombinant caspase-3 (Figure 4c).

Caspase-3 inhibition was confirmed by biochemical analysis. Protein samples harvested from neurons incubated with
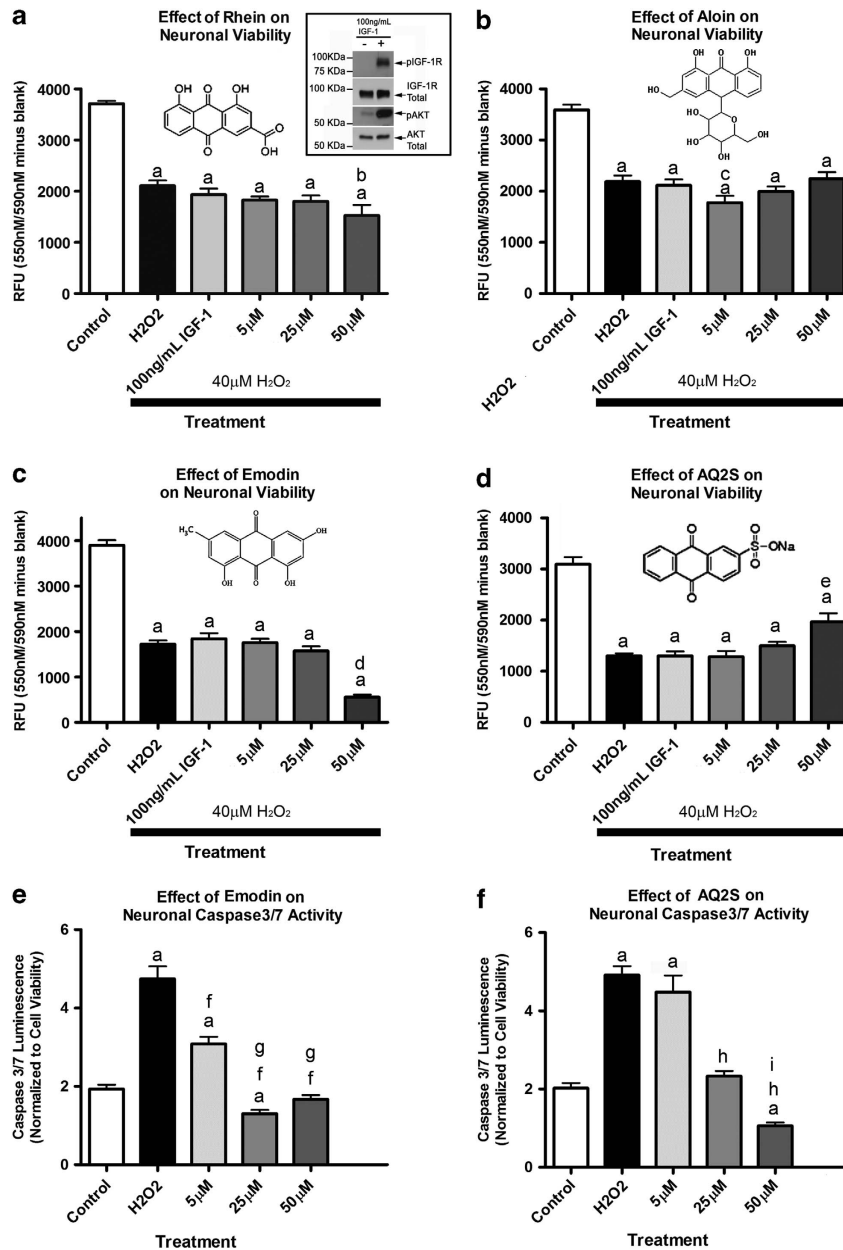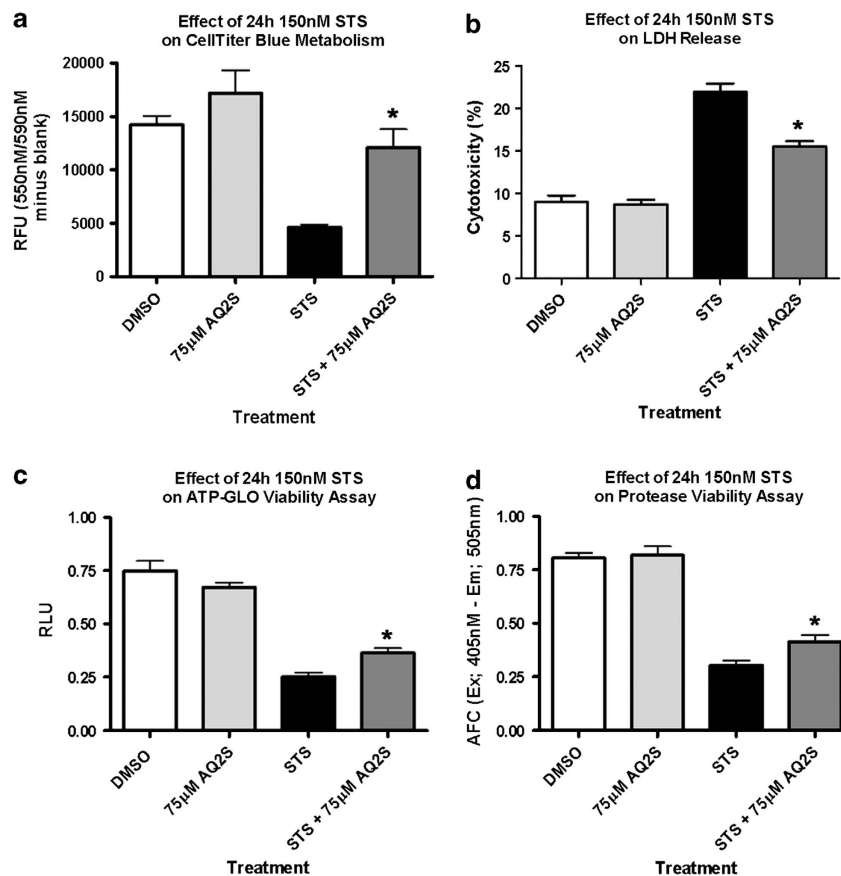
Figure 1 Effect of anthraquinones on H2O2 Injury. Primary rat cortical neurons were seeded onto a 96-well plate. (**a**) The effect of 100 ng/ml IGF-1 and rhein on 24-h neuronal death. Validation of IGF-1 stimulation (boxed western blot insert—upper right). Both IGF-1R and Akt are activated after 25-min stimulation with 100 ng/ml IGF-1 in 2-h supplement starved cortical neurons. (**b**) The effect of 100 ng/ml IGF-1 and aloin on neuronal death. (**c**) The effect of 100 ng/ml IGF-1 and emodin on neuronal death. (**d**) The effect of 100 ng/ml IGF-1 and AQ2S on neuronal death. (**e**) The effect of emodin on H2O2-induced caspase 3/7 activation. (**f**) The effect of AQ2S on H2O2-induced caspase 3/7 activation. Horizontal black bars indicate groups treated with 40 μM H2O2. Data was analyzed using one-way-ANOVA ($n = 8$/treatment; $P < 0.0001$; graphs show mean + S.E.M.). Letters indicate significant results of Fisher LSD *post-hoc* test. **a** = compared with no injury DMSO control (white bar) **b** = compared with injury only DMSO (black bar) and IGF-1, **c** = compared with injury only DMSO (black bar) and 50 μM aloin, **d** = compared with injury only DMSO (black bar), IGF-1, 5 emodin, and 25 μM emodin, **e** = compared with injury only DMSO (black bar), IGF-1, and 5 μM AQ2S, **f** = compared with injury only DMSO (black bar), **g** = compared with 5 μM emodin, **h** = compared with injury only DMSO (black bar), **i** = compared with 25 μM AQ2S

125 μM AQ2S and 500 nM STS for 6 h were run on western blot. Consistent with caspase-3 inhibition, cleaved (i.e., activated) capase-3 was reduced in AQ2S-treated neurons (Figure 4d). Finally, we biochemically confirmed the inhibition of caspase-3 by AQ2S via western blot analysis of substrate cleavage products. Poly ADP ribose polymerase is a classic caspase-3 substrate. The parent protein migrates at ∼116

KDa on SDS-PAGE. An 89-KDa product is produced upon cleavage by caspase-3. Cortical neurons were subjected to 250 nM STS for 6 h. 125 μM AQ2S significantly reduced the formation of the 89-KDa species (Figures 4e and f). Furthermore, 125 μM AQ2S reduced loss of the NF-κB p65 subunit (another caspase-3 target[32,33]) after 17 h 250 nM STS (Supplementary Figure 5).

a

Effect of AQ2S on
Neuronal Viability

b

Effect of AQ2S on
Neuronal Caspase3/7 Activity
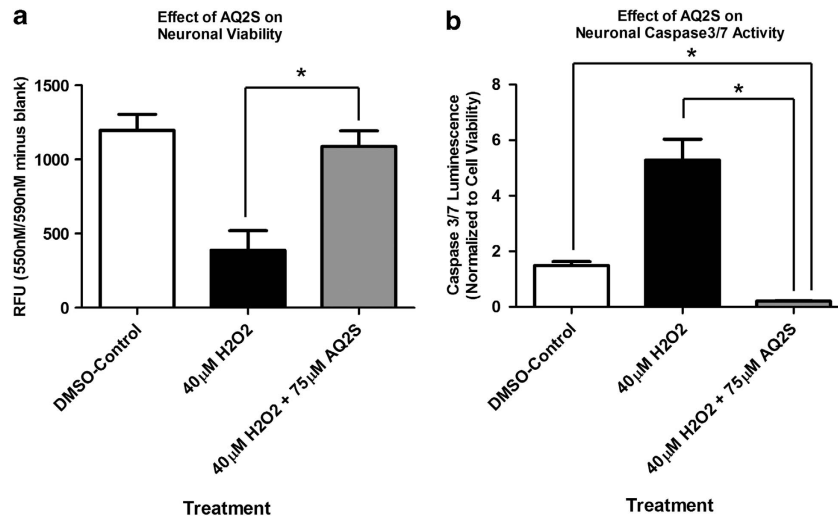
Figure 2 Enhanced protection against H2O2 injury by high-concentration Aq2s. Primary rat cortical neurons were seeded onto a 96-well plate. (**a**) The effect of AQ2S on neuronal viability. (**b**) The effect of AQ2S on H2O2-induced caspase 3/7 activation. Caspase results were transformed to log(Y) values and analyzed using one-way-ANOVA ($n = 8$/treatments; $P < 0.0001$; graphs show mean + S.E.M.). Viability was analyzed using one-way-ANOVA ($P < 0.0001$). Asterisks (*) indicate Fisher LSD *post-hoc* significance

a

Effect of 24h 150nM STS
on CellTiter Blue Metabolism

b

Effect of 24h 150nM STS
on LDH Release

c

Effect of 24h 150nM STS
on ATP-GLO Viability Assay

d

Effect of 24h 150nM STS
on Protease Viability Assay

Figure 3 AQ2S prevents STS-induced neuronal death. Primary rat cortical neurons were seeded onto 96-well plates. The effect of + 150 nM STS and + 75 μM AQ2S on 24-h neuronal viability and cell death as quantified by (**a**) celltiter Blue ($n = 6$/treatment group), (**b**) LDH release ($n = 8$/treatment group), (**c**) viability-GLO ATP assay ($n = 10$/no injury groups; $n = 9$/STS injury groups), and (**d**) live-cell protease activity ($n = 8$/treatment group). Assays were analyzed using one-way-ANOVA ($P < 0.0001$; graphs show mean + S.E.M.). Asterisks (*) indicate significance with Fisher's LSD *post-hoc* test
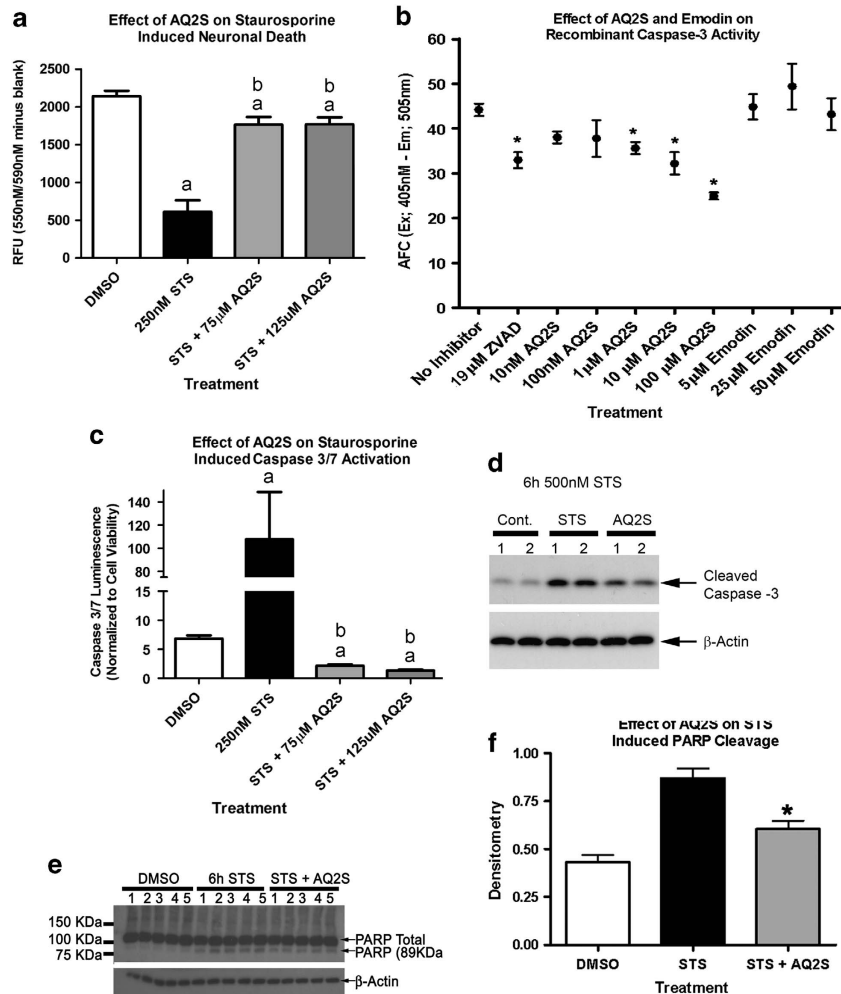
Figure 4 AQ2S is a direct caspase-3 inhibitor. Primary rat cortical neurons were seeded onto a 96-well plate. (**a**) The effect of 24 h 250 nM STS on neuronal viability in the absence or presence of AQ2S ($n = 7$/STS control injury, $n = 8$/all other treatments). (**b**) The effect of AQ2S, Emodin, and ZVAD-fmk to inhibit recombinant activated caspase-3 as determined by inhibition of free AFC in a 96-well in vitro assay ($n = 7$/no inhibitor, $n = 8$/ZVAD-fmk, $n = 4$ all other treatment groups). (**c**) The effect of 24 h 250 nM STS on neuronal caspase 3/7 activity the absence or presence of AQ2S ($n = 7$/STS control injury, $n = 8$/all other treatments). (**d**) Biochemical validation of caspase-3 inhibition in neurons after 6 h 500 nM STS + 125 μM AQ2S ($n = 2$/treatment). (**e**) PARP cleavage in neurons after 6 h 250 nM STS + 125 μM AQ2S ($n = 5$/treatment). (**f**) Densitometry of 89-KDa PARP cleavage fragment in STS + AQ2S-treated cells ($n = 5$/treatment). Neuronal viability data, caspase-3 drug screening assay data, and PARP cleavage data were analyzed using one-way-ANOVA ($P < 0.0001$; graphs show mean + S.E.M.). Neuronal caspase-3 data was transformed to log(Y) values and analyzed using one-way-ANOVA ($P < 0.0001$ graphs show mean + S.E.M.). Letters and asterisks indicate significant ($P < 0.05$) results of Fisher LSD post-hoc test. **a** = compared with no injury DMSO control (white bar). **b** = compared with injury only DMSO (black bar). Data was analyzed using one-way-ANOVA ($P < 0.0001$; graphs show mean + S.E.M.)

We next determined if AQ2S inhibits other caspases. Incubation of cortical neurons with 150 nM STS significantly increased caspase-3, caspase-8, and caspase-9 activity at 24 h. Co-treatment with 75 μM AQ2S significantly reduced baseline and injury activity levels of all three caspases (Figure 5). However, 75 μM AQ2S showed greatest potency against caspase-3.

AQ2S does not interfere with the luciferase reaction.
The in vitro caspase 3, 8, and 9 activity assays (Promega, Madison, WI, USA) utilize luminescence as a proxy for enzyme activity. Although a powerful technique, the inhibition of luciferase signal by chemical interference (false-positive) can be problematic.[34,35] Artifact-dependent inhibition of luminescent signal occurs via three primary mechanisms.

(1) Redox cycling of a chemical interferes with the oxidation of luciferin substrate. (2) Production of reactive radical species by redox active chemicals destroys the luciferase enzyme. (3) Colored/fluorescent compounds interfere with luciferase signal detection.

AQ2S is used to study the redox cycling behavior of anthraquinones.[36] In addition, dissolved in DMSO, AQ2S presents a faint-yellow hue. To verify that AQ2S-mediated inhibition of caspase3/7 luminescence on the H_2O_2/STS assays were not artifacts, we compared the effect of AQ2S at different concentrations on two-cell viability tests (one fluorometric and the other luminescent). AQ2S was incubated at 25, 50, 75, or 125 μM for 24 h. After 24 h, the respective cell viability reagent was added and cell survival assayed. As measured by the fluorometric CellTiter Blue assay, none of
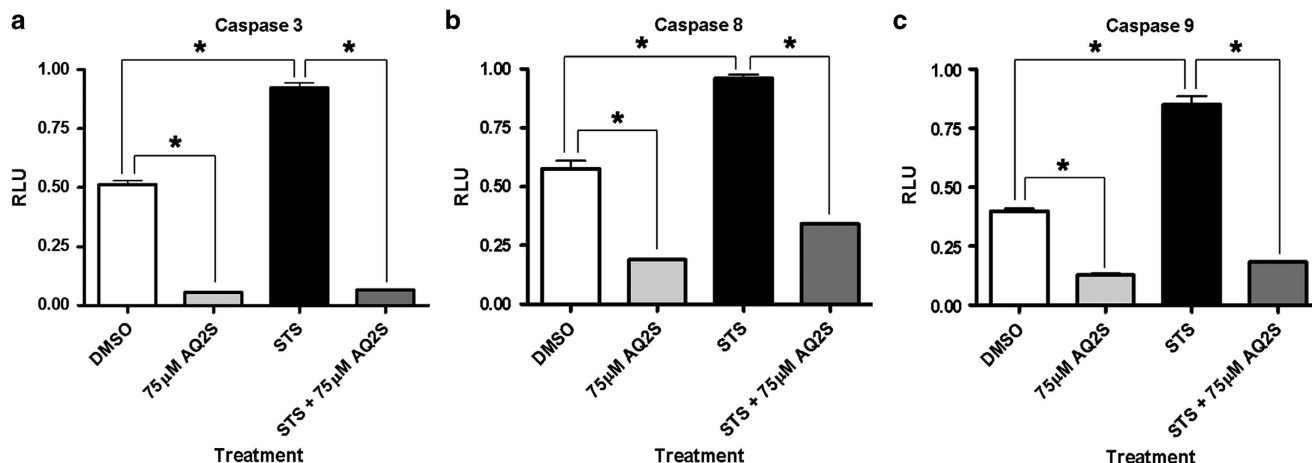
Figure 5 AQ2S inhibits initiator and executioner caspases. Primary rat cortical neurons were seeded onto 96-well plates. Neurons were treated with + 150 nm STS and + 75 μM AQ2S for 24 h. Graphs show caspase activity (relative luminescent units, RLU) for (**a**) caspase-3/7 ($n = 6$/treatment group) (**b**) caspase-8 ($n = 6$/treatment group), and (**c**) caspase-9 ($n = 6$/treatment group). Data was analyzed using one-way-ANOVA ($P < 0.0001$ for all graphs; graphs show mean + S.E.M.). Asterisks indicate significant ($P < 0.05$) results of Fisher LSD *post-hoc* test

the AQ2S concentrations used inhibited viability below control levels (Supplementary Figure 6A). Similar results were observed using the luminescent viability-GLO assay (Supplementary Figure 6B). Finally, to replicate the exact experimental conditions used in injury studies, neurons were first incubated with the CellTiter Blue reagent for 2 h. Subsequently, the viability-GLO reagent was added for 1 h and luminescence measured (i.e., viability reagents were mixed together; Supplementary Figure 6C). When both assays were combined, AQ2S caused a slight (~ 13–17%) decrease in luminescent signal compared with DMSO controls. The data support that AQ2S is a novel caspase inhibitor.

AQ2S activates the pro-survival kinase AKT. AKT is a key pro-survival kinase that is dysregulated by acute brain injury.[37] Many diverse therapies used to prevent neuronal death activate AKT, including small molecules,[38] endogenously derived survival proteins,[39,40] and other non-pharmacology based treatments like therapeutic hypothermia.[41–43] To further elucidate the mechanisms of AQ2S-mediated neuroprotection, the level of activated (phosphorylated) AKT was measured by western blot.

AQ2S-mediated AKT activation was first assayed under non-injury conditions. 125 μM AQ2S was added to fresh neurobasal/B27 media and incubated for 4 and 24 h. AQ2S induced a significant (but modest) rise in pAKT473 after 4-h treatment (Figures 6a, c and e). No effect on AKT total was observed (Figure 6d). Alternatively, the effect of AQ2S on pAKT473 was not significant at 24 h (Figure 6b).

We tested if AQ2S increased pAKT473 after STS injury. We compared the effects of AQ2S and emodin to modulate pAKT473 after 6 h 250 nM STS. STS alone induced AKT activation. AQ2S marginally increased STS-induced pAKT473 at the 6-h time point, but did not reach statistical significance. Alternatively, 50 μM emodin abolished baseline and injury induced AKT activation (Figures 7a and b).

We determined if longer exposure to AQ2S increased AKT activation. Cortical neurons were co-treated with 125 μM

AQ2S and 250 nM STS for 17 h. AQ2S-treated neurons showed a significant elevation in pAKT473 after 17 h STS injury (Figures 8a and b). Furthermore, total AKT levels were significantly reduced in all STS-treated groups (Figures 8a and c). Therefore, consistent with the 6-h observation, compared with non-injured controls, the ratio of pAKT473/AKT was slightly elevated with STS injury alone (although it did not reach significance at this time point Figure 8d). To determine the specificity of AQ2S-mediated signaling changes, extracellular-regulated kinase (ERK) was also examined. 17 h STS abolished ERK activation. AQ2S treatment did not prevent STS-mediated ERK inhibition. Moreover, total ERK levels did not change (Figure 8a).

To determine if AKT activation is critical for AQ2S-mediated neuroprotection, neurons were injured with 250 nM STS in the absence or presence of 125 μM AQ2S and 10 μM LY294002 (PI3K/AKT inhibitor) for 21 h. Consistent with previous observations, pAKT473 and pERK levels were decreased by STS injury. In addition, pAKT473 increased in the presence of AQ2S, and AQ2S-induced pAKT473 was blocked by LY294002 (Figure 9a). However, after 24-h 250-nM STS injury, LY294002 failed to block AQ2S-mediated neuroprotection (Figure 9b).

Finally, we compared the protective effect of AQ2S to other documented neuroprotectants. 250 nM STS was co-administered with minocyline, AQ2S, IGF-1 or ZVAD for 24 h. Only ZVAD and AQ2S increased cell viability after 24 h (Figure 10). Neither minocycline nor IGF-1 reduced neuronal death. However, 24 h of IGF-1 pre-treatment is neuroprotective and reduces a subsequent 24 h STS injury (data not shown).

AQ2S does not promote lipid peroxidation. Many quinone species are toxic redox cycling chemicals and increase the level of reactive radicals.[44] In turn, reactive radicals promote lipid peroxidation and cause cellular damage. To test if AQ2S promotes lipid peroxidation in neurons, at D.I.V. 12, culture media was exchanged with Neurobasal/B27 (-AO) in the absence or presence of 125 μM AQ2S for 48 h. D.I.V. 14 neurons were harvested and analyzed for 4-HNE
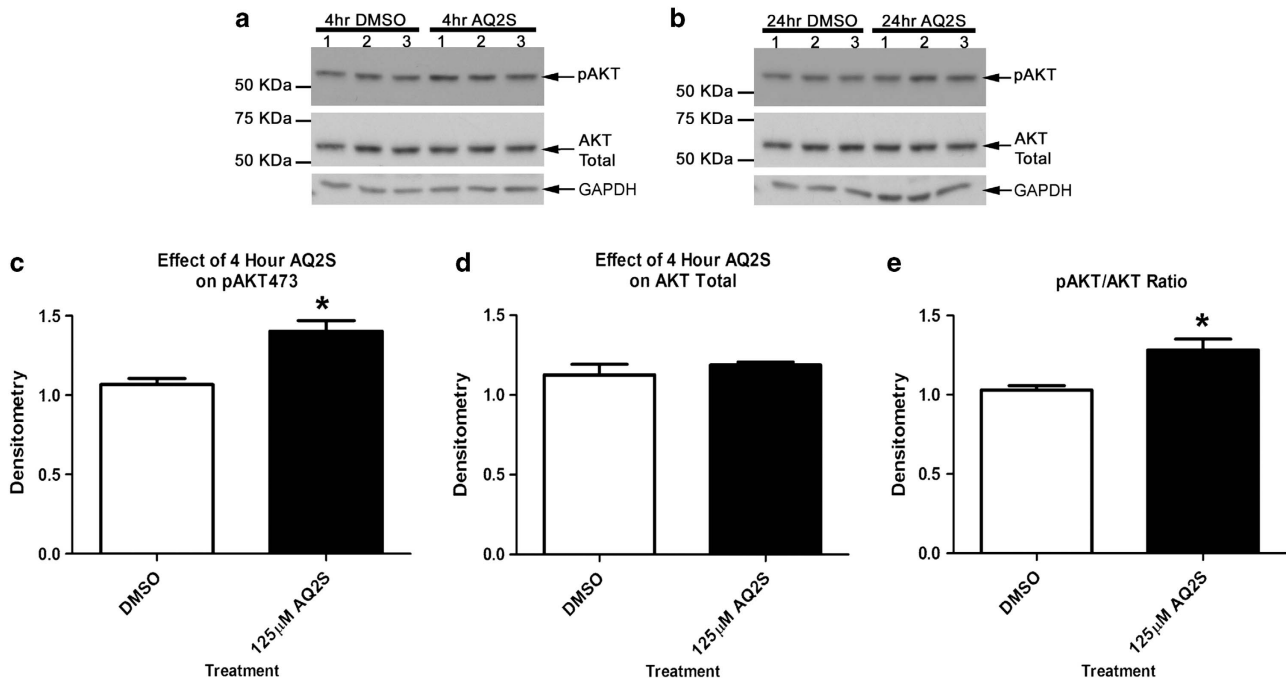
Figure 6 AQ2S activates Akt under baseline conditions. Primary rat corticalneurons were seeded onto six-well plates. Cells were treated with or without AQ2S in triplicate. (**a**) Blots show the effect of AQ2S on pAKT473 and AKT total levels after a 4-h treatment. (**b**) Blots show effect of AQ2S on pAKT473 and AKT total levels after a 24-h treatment. Densitometric semiquantification of (**c**) 4 h pAKT473 and (**d**) 4 h AKT total levels. (**e**) Ratio of 4 h pAKT473/AKT total. Data was analyzed using unpaired t-test ($n = 3$/treatment; pAKT473, $P = 0.0124$; pAKT/AKT ratio, $P = 0.0278$; graphs show mean + S.E.M.). Asterisks (*) indicate significance

levels. AQ2S did not significantly increase the basal level of 4-HNE (unpaired t-test, $P = 0.1856$; Figure 11a).

Injury (e.g., brain ischemia), robustly increases endogenous reactive oxygen species, which may promote the formation of deleterious quinone radicals and increase lipid peroxidation. We tested if lipid peroxidation induced by 200 μM H_2O_2 is enhanced by AQ2S. D.I.V. 13 neurons were treated for 4.5 h with 200 μM H_2O_2 in fresh neurobasal/B27 (-AO) in the presence or absence of 125 μM AQ2S. 200 μM H_2O_2 increased 4-HNE levels. The asterisk indicates a ~40–45-KDa band, particularly, sensitive to treatment. AQ2S did not significantly upregulate 4-HNE staining after a 4.5-h incubation (unpaired t-test; $P = 0.0901$; Figure 11b).

Discussion

Post-treatment with emodin is not neuroprotective. Recent studies indicate that natural AQs prevent neuronal death. Contrary to these findings, administered after H_2O_2 injury, we report that emodin, rhein, and aloin are not beneficial. In primary neurons, we found that 50 μM emodin exacerbates injury, and rapidly inhibits basal AKT activation. Our data suggest that emodin is toxic to neurons. Exposing neurons to non-lethal doses of toxic agents is neuroprotective.[45] Emodin induces reactive oxygen species-mediated cell death in lung adenocarcinoma cells,[19] and it increases caspase 3/7 activation in BV-2 cells.[46] Preconditioning responses may partially explain why pre-treatment with emodin is neuroprotective in other neuron culture studies.[10]

We found that emodin reduced caspase-3 activity (Figure 1) in neurons but it was not a direct caspase inhibitor in the cell-free assay (Figure 4). Studies show that high H_2O_2 concentrations can inhibit caspase-3 activation.[47] 24 h emodin may have exacerbated oxidative stress in our system and inhibited caspase-3 by indirect mechanisms (explaining the discrepancy in Figures 1 and 4). Caspase-3 inhibition via oxidative mechanisms would not prevent necrosis.[48] Moreover, 50 μM emodin may have potentiated cell death by reducing AKT473 levels in cortical neurons; synergizing with H_2O_2-induced impairment of IGF-1/AKT survival signaling.

AQ2-mediated mechanism(s) of neuroprotection. AQ2S was reproducibly neuroprotective in the H_2O_2 assay (Figures 1 and 2). To understand the mechanisms of protection, we first analyzed caspase-3. It blocked injury induced caspase-3 activation, and reduced activity below baseline non-injured levels. Moore et al.([49]) examined the neuroprotective effect of BAF (pan-caspase inhibitor) on primary rat cortical neurons injured with either 24 h STS, C2-ceramide, camptothecin, N-methyl-D-aspartic acid, or H_2O_2. BAF reduced cell death in every model where caspase was activated except H_2O_2.[49] The finding suggests that caspase inhibition alone is insufficient to protect after H_2O_2 injury. Thus, AQ2S may activate caspase-independent survival mechanisms after oxidative injury as well.

AQ2S reproducibly protected neurons in the STS assay (Figures 3, 4, 9 and 10). It inhibited multiple caspases, reduced poly ADP ribose polymerase cleavage, and directly interfered with active caspase-3 on a cell-free assay. Thus

a

b
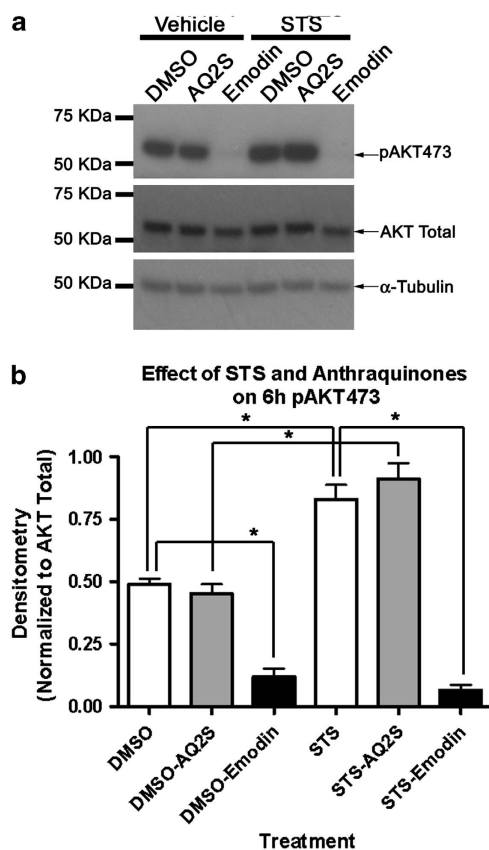
Figure 7 Emodin blocks acute STS-induced AKT activation. Primary rat cortical neurons were seeded onto six-well plates. Neurons were treated with 125 μM AQ2S or 50 μM Emodin + 250 nM STS for 6 h. (**a**) Representative western blots show emodin, but not AQ2S, inhibits AKT activity. (**b**) Densitometry of western blots ($n = 4$/treatment group). Data was analyzed using one-way-ANOVA ($P < 0.0001$ for all graphs; graphs show mean + S.E.M.). Asterisks indicate significant ($P < 0.05$) results of Fisher LSD *post-hoc* test

AQ2S is a novel caspase inhibitor. 75 and 125 μM AQ2S equally protected against 250 nM STS (Figure 4). This may be explained by almost total caspase-3 inhibition at both concentrations. In our system, AQ2S barely induced neuroprotection under high STS (500 nM) conditions. Deshmukh and Johnson[31], using *in vitro* primary rat sympathetic neurons, report that low concentrations of STS (100 nM) for 48 h induce caspase-dependent cell death, while high STS concentrations for 48 h (500 and 1000 nM) activate caspase-independent cell death pathways. BAF prevented neuronal death at 100 nM STS but not at the 500 and 1000 nM concentrations.[31] Thus, in our STS model, AQ2S did not block caspase-independent cell death mechanisms activated by 500 nM STS.

To further elucidate the neuroprotective mechanisms of AQ2S, we tested if the pro-survival kinase AKT was involved. We observed that AQ2S potently stimulates AKT activity under STS injury conditions at 17 (Figure 8) and 21 h (Figure 9), but not at 6 h (Figure 7). Furthermore, AQ2S only mildly activates AKT under non-injury conditions (4 h; Figure 6). Unexpectedly however, preventing AKT activation with LY294002 failed to abolish AQ2S's neuroprotective action after STS injury (Figure 9). One explanation is that

caspase inhibition is sufficient to achieve neuroprotection after STS injury (hence protection by ZVAD). Nevertheless, studies show that overexpression of constitutively active AKT also prevents STS-induced cell death in a dorsal root ganglion cell line.[50] Therefore AKT activation is neuroprotective in the STS injury model — indicating that AQ2S is activating multiple-survival mechanisms.

AQ2S is a non-toxic quinone with unique redox properties. AQ2S is a synthetic AQ used in wood pulping,[51,52] and the basis for many AQ dyes.[53] Given the focus on industrial utilities, few studies have examined AQ2S in biological systems. We expected AQ2S to behave as a toxic agent[54,55] and emodin to exert neuroprotective actions. Unexpectedly, the opposite was achieved. Not only was AQ2S safe, it protected neurons from oxidative and chemical injury. We are the first to show that AQ2S prevents cellular injury. Although much remains to be elucidated concerning the mechanisms of action, prior work does provide some insight into why AQ2S is uncharacteristically (for a quinone) non-toxic.

A primary danger of quinone compounds in biological systems is that highly reactive by-products/intermediates are produced from their metabolic biotransformation. Bayol-Denizot *et al.*[56] investigated the metabolism of AQ2S by NADPH-cytochrome *P*450 reductase in primary rat neurons, astrocytes, and cerebral endothelial cells. *In vitro* incubation of 980 μM AQ2S significantly upregulated the toxic metabolic bi-product superoxide anion (O_2^-) in all three cell types over 60 min. Importantly, the authors found that AQ2S-induced O_2^- was blocked by co-incubation with the endogenous antioxidant SOD. However, SOD was incapable of fully blocking O_2^- produced by menadione, another xenobiotic under study.[56] These findings indicate that the metabolic redox chemisty for AQ2S is different than other xenobiotics. Moreover, the authors noted that AQ2S did not induce cell death at 980 μM.

AQ2S also showed unique redox properties in studies by Winterbourn.[57] The ability of semiquinone radicals to donate electrons (i.e., reduce) cytochrome *c* was examined.[57] All quinones tested, including AQ2S, reduced cytochrome *c* if in radical form. However, addition of SOD and molecular oxygen (O_2) to the reaction prevented AQ2S-mediated cytochrome *c* reduction. This observation was only found for AQ2S but not menadione, benzequinone, and several other napthroquinones. Winterbourn hypothesized that AQ2S prefers the oxidized (non-radical) state, because of its negative redox potential (AQ2S; $E^o = -0.39$). In the presence of molecular oxygen (O_2; $E^o = -0.17$), AQ2S is a less attractive electron acceptor. Thus, the majority of electrons remain with O_2 to form O_2^- radicals, and are rapidly eliminated by SOD (preventing cytochrome *c* reduction). Consistent with these reports on AQ2S, we observe little effect of AQ2S to inhibit luminescence signal by redox artifacts (Supplementary Figure 6B) or increase cellular 4-HNE levels (Figure 11), indicating that either AQ2S is a mild redox agent in the biological system or radical production is efficiently managed by endogenous neuronal scavenging systems (e.g., SOD).

Metabolism of quinones can increase reactive oxygen species and lead to toxic lipid peroxidation. This can have important clinical implications. For example, doxorubicin
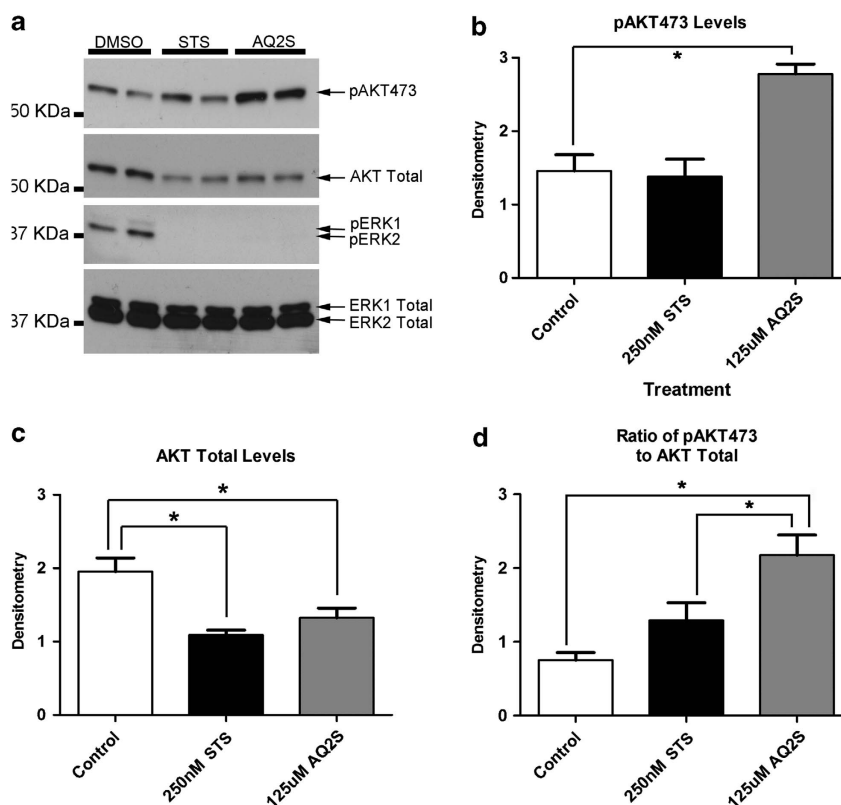
Figure 8 AQ2S activates AKT after long-term STS exposure. Primary rat cortical neurons were seeded onto six-well plates. Cells were treated with STS + AQ2S ($n = 4$/treatment). (**a**) Representative western blots ($n = 2$) showing the effect of STS and STS/AQ2S on pAKT473, AKT Total, pERK1/2, and ERK1/2 total levels. Densitometric semiquantification of (**b**) pAKT473 and (**c**) AKT total levels. (**d**) Ratio of pAKT473/AKT total. Data was analyzed using one-way-ANOVA ($n = 4$/treatment; pAKT, $P = 0.0254$; AKT total, $P < 0.0001$; pAKT/AKT ratio, $P = 0.0032$; graphs show mean + S.E.M.). Asterisks (*) indicate Fisher LSD post-hoc significance

(DOX) is an anthraquinone-based chemotherapeutic agent. The primary limitation of DOX therapy for the treatment of cancer is cardiotoxicity due to lipid peroxidation.[58] In our study, AQ2S did not raise 4-HNE levels. The absence of increased lipid peroxidation suggests that AQ2S may be a metabolically safe/well-tolerated AQ. Consistent with this idea, Vile and Winterbourn ([59]) found that AQ2S unexpectedly inhibited Fe^{3+}-induced lipid peroxidation in rat liver microsomes (as measured by thio-barbituric acid-reactive products). The authors lacked a mechanistic explanation for the observation but inferred that AQ2S may interfere with redox processes downstream of Fe^{3+} reduction that cause lipid peroxidation.[59]
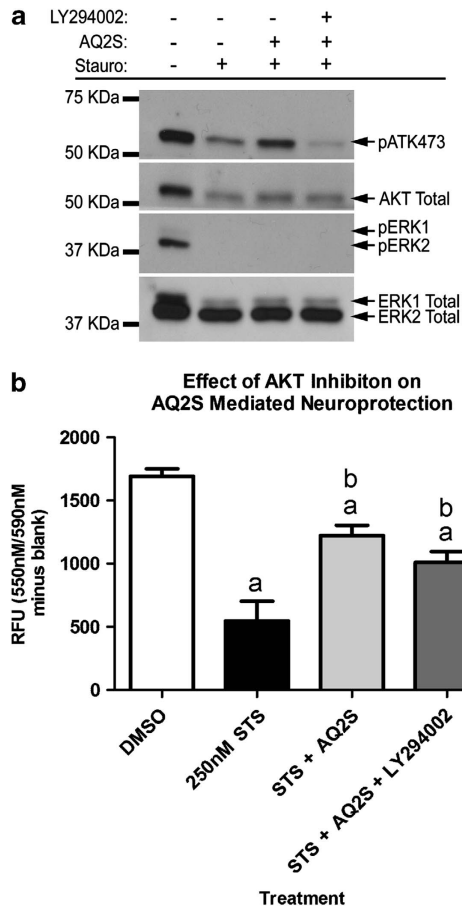
Conclusions

We discovered that the synthetic quinone AQ2S potently prevents death of primary neurons. Our work indicates that AQ2S is a lead compound to develop a novel neurotherapeutic AQ-based drug. The mechanism(s) of neuroprotection involve caspase inhibition and AKT activation. In addition, AQ2S is effective when given after injury (post-treatment). This could have important implications for the treatment of acute CNS injuries such as traumatic brain injury, stroke, and cardiac arrest. Future studies need to further elucidate the mechanisms of action, and test if AQ2S is neuroprotective in clinically relevant in vivo brain injury paradigms.

Materials and Methods

Animals. E17-E19 rat embryos were harvested from timed pregnant Sprague Dawley (SD) rats (Charles River). Pregnant rats were sacrificed by isoflurane overdose and immediately decapitated to ensure euthanasia before embryo collection. All animal work was approved by the Institutional Animal Care and Use Committee of the University of Pittsburgh. The described protocol adheres to recommendations established by the American Medical Veterinary Association Guideline for Euthanasia. Rats were euthanatized as to eliminate pain and suffering, and the minimal number of animals used for these studies.

Experimental compounds. Emodin ($>90\%$ pure), rhein ($>98\%$ pure), aloin ($>97\%$ pure), and aq2s (97% pure) were all purchased from Sigma. LY294002 ($<99\%$ pure), STS ($>98\%$ pure), minocycline hydrochloride ($>98\%$ pure), and ZVAD-fmk (95% pure) were purchased from Tocris (Bristol, UK). Human recombinant IGF-1 was purchased from Peprotech (Rocky Hill, NJ, USA). All compounds were dissolved in DMSO and stored in 1.5-ml light-protected tubes.

Neuronal cell culture. Cultures were maintained using our previously published techniques that yield a 95% enriched neuron population.[60] Briefly, brains were isolated from E18-19SD rat embryos. Embryonic cortical brains were dissected in ice cold buffer solution under a microscope (Leica M651, Buffalo Grove, IL, USA). Cortical halves were collected in a 1.5-ml centrifuge tube and rapidly minced over a 2-min period using sterile scissors. Tissue was spun at 4 °C/200 g/5 min and pellet trypsinized in a water bath for 8 min. Dissociated cells were spun at 4 °C/200 g/5 min and triturated. Neurons were resuspended in prepared plating media (neurobasal/B27 supplemented with 25 μM glutamic acid). Neurons were counted using a hemacytometer and plated at high density ($\sim 1.2 \times 10^6$/well of a six-well plate; $\sim 1.5 \times 10^5$/well of a 96-well plate) on poly-D-lysine coated plates (BD Biosciences, San Jose, CA, USA). Every 3 days, half the media was exchanged with fresh neurobasal/B27 (Life Technologies, Grand Island, NY, USA). On D.I.V.3, 8 μM cytosine β-D-arabinofuranoside hydrochloride was added to prevent glial proliferation. Experiments were performed between days in vitro (D.I.V.) 7–14.

a

LY294002:	-	-	-	+
AQ2S:	-	-	+	+
Stauro:	-	+	+	+

75 KDa

50 KDa   ← pATK473

50 KDa   ← AKT Total

37 KDa   ← pERK1 / ← pERK2

37 KDa   ← ERK1 Total / ← ERK2 Total

b

Effect of AKT Inhibiton on AQ2S Mediated Neuroprotection

Y-axis: RFU (550nM/590nM minus blank)

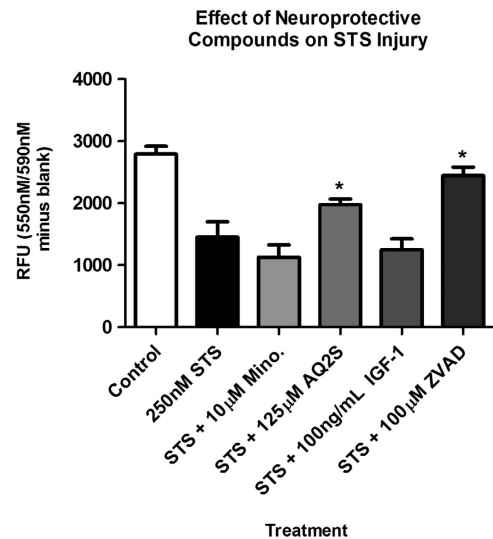Treatment: DMSO, 250nM STS, STS + AQ2S, STS + AQ2S + LY294002

Figure 9 Blocking AKT does not prevent AQ2S-mediated neuroprotection. Primary rat cortical neurons were seeded onto a six-well plate. (**a**) Western blots validate the effect of LY294002 to block AQ2S-mediated AKT activation. (**b**) Effect of AQ2S alone or in combination with LY294002, to prevent 24 h 250 nM STS-induced neuronal death. Data was analyzed using one-way-ANOVA ($n = 6$/treatment; $P < 0.0001$; graphs show mean + S.E.M.). Letters indicate significant results of Fisher LSD post-hoc test. **a** = compared with DMSO control (white bar), **b** = compared with injury only DMSO (black bar)

H₂O₂ injury. Cortical neurons were harvested and plated in neurobasal/B27 (with antioxidants; + AO). Neurons were switched to neurobasal/B27 minus antioxidants (− AO) after D.I.V. 3. Fresh media was exchanged by half-media replacement at D.I.V. 3, 6, 9. H_2O_2 was prepared fresh before each injury experiment. At D.I.V 10, 30% concentrated H_2O_2 (Sigma) was first diluted in sterile ddH₂O. Diluted stock H_2O_2 was directly added to unprepared (no B27 supplement) neurobasal media at the desired final concentration. Growth maintenance media was aspirated from neurons in 96-well format, and replaced with 150 μL neurobasal media containing H_2O_2 incubated for 35 mins. Following injury, neurobasal/H_2O_2 media was aspirated and replaced with 100 μL fresh neurobasal/B27 (− AO) containing DMSO only or drug treatments at desired concentrations for 24 h.

STS injury. Cortical neurons were harvested and plated in neurobasal/B27 (+ AO). At D.I.V. 7–11, half media was collected (conditioned media) and mixed with an equal volume fresh neurobasal/B27 (to make the 24-h treatment media). STS was prepared at the desired concentration in treatment media, with or without experimental drugs. The remaining growth maintenance media was replaced with 100 μL of treatment media per well of a 96-well plate (or 2 ml for a six-well plate) for 24 h.

Cell viability assays. All assays were prepared according to the vendor's instructions. Briefly, 24-h post-injury, 20 μL CellTiter Blue (Promega) was directly added to each well of a 96-well plate. Plates were incubated in the dark for ∼ 2 h,

Effect of Neuroprotective Compounds on STS Injury

Y-axis: RFU (550nM/590nM minus blank)

Treatment: Control, 250nM STS, STS + 10 μM Mino., STS + 125 μM AQ2S, STS + 100ng/mL IGF-1, STS + 100 μM ZVAD

Figure 10 Comparison of AQ2S and ZVAD protect against STS injury. Primary rat cortical neurons were seeded onto a 96-well plate. Cortical neurons were incubated 24 h with DMSO (control), 250 nM STS (injury only), STS + 10 μM minocycline, STS + 125 μM AQ2S, STS + 100 ng/ml IGF-1, or STS + 100 μM ZVAD (all groups $n = 8$/treatment except ZVAD $n = 7$/treatment). Viability assays were analyzed using one-way-ANOVA ($P < 0.0001$; graphs show mean + S.E.M.). Asterisks (*) indicate significance with Fisher LSD post-hoc test

and metabolism of resazurin measured using a fluorometric plate reader (Fusionα, Packard/PerkinElmer, Waltham, MA, USA). In separate experiments, 100 μL of CellTiter-GLO assay reagent (Promega) was added directly to each well of a 96-well plate as a terminal procedure (neurons are lysed). ATP levels in live cells increase luminescence and was measured using a luminometer (Wallac 1420 Victor II multiwell counter, PerkinElmer Life Sciences). In separate experiments, 100 μL of CellTiter-Fluor assay reagent (Promega) was added directly to each well of a 96-well plate. Live-cell protease activity was measured by detection of free AFC reagent.

Caspase-GLO luminescent assay. Caspase3/7-GLO regent (Promega) can be multiplexed with the CellTiter Blue viability assay. 100 μL caspase3/7-GLO reagent was directly added to each well of a 96-well plate as a terminal procedure (neurons are lysed) and incubated for 1 h. Luminescence was measured using a luminometer. In separate experiments, 100 μL caspase 8-GLO and Caspase 9-GLO reagents were added to each well of a 96-well plate.

Lactate dehydrogenase (LDH) assay. The LDH Cytotoxicity Assay Kit II was purchased from Abcam (Cambridge, MA, USA). Neurons were cultured in 96-well format and subjected to STS injury ± AQ2S for 24 h (in 100 μL total media volume). At 23-h maximum LDH release (positive control) was prepared by adding 10 μL cell lysis reagent directly to a few non-injured wells (i.e., no STS or AQ2S). At the end of the 24-h injury period, 80 μL of media was transferred to a new 96-well plate. Plates were spun at ∼ 500 g for 5 mins. 10 μL of cell culture treatment media was added to a new black-walled plate and advanced WST detection reagent added. The mix was incubated for ∼ 15 min and absorbance measured (OD 450 nm). Fresh culture media was used as a negative control. Cytotoxicity was calculated using the standard formula: cytotoxicity % = (sample LDH—negative-control LDH)/(maximum LDH release—negative-control LDH) *100.

TUNEL analysis. Neurons were grown on poly-ᴅ-lysine/laminin eight-well culture slides (BD Biosciences). Neurons were treated with 50 μM H_2O_2. After 24-h injury, wells were rinsed once in ice cold PBS, and incubated in 4% paraformaldehyde for 25 mins at 4 °C. Slides were prepared for TUNEL analysis using vendor kit/protocol (Dead End Fluorometric TUNEL kit; Promega). Slides were mounted in solution containing DAPI. TUNEL positive nuclei glow green under fluorescent microscope (Eclipse 50, Nikon, Melville, NY, USA). Data were collected and analyzed as follows: Three random field images were collected from

a

Minus AO's 48 Hours

b

200 μM H2O2 4.5 Hours
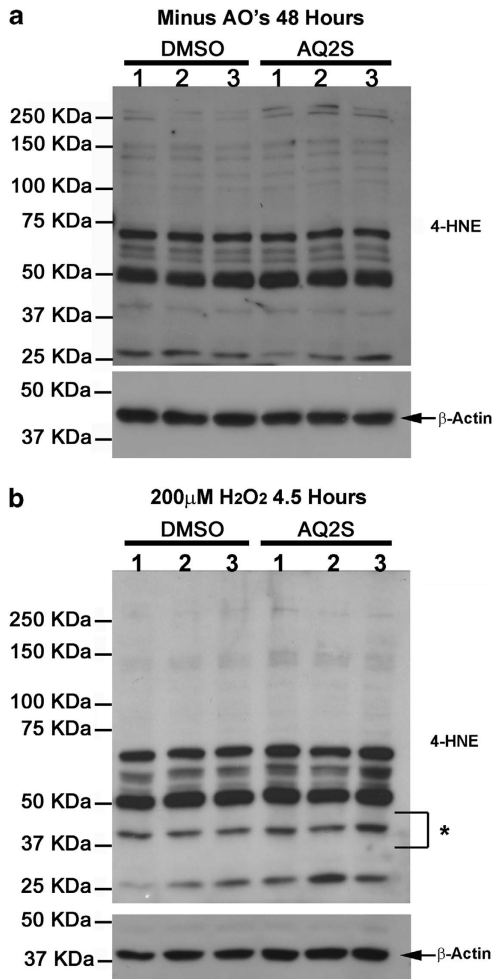
Figure 11 AQ2S does not promote lipid peroxidation in neurons. Primary rat cortical neurons were seeded onto six-well plates. Cells were treated in triplicate. (**a**) Western blots show the level of 4-HNE in neurons treated 48 h with or without 125 μM AQ2S in B27–AO media. (**b**) Representative blots show 4-HNE levels in neurons treated 4.5 h with 200 μM H2O2 in the absence or presence of 125 μM AQ2S in B27–AO media. Asterisk indicates a ∼ 40–45-KDa band sensitive to injury. Densitometric semiquantification of entire 4-HNE lanes were measured and normalized to β-actin (graphs not shown) Data was analyzed using unpaired *t*-test. (*n* = 3/treatment; 48 h 4-HNE, *P* = 0.1856; 200 μM H2O2 4-HNE, *P* = 0.0901)

a single well of an eight-well culture slide under 20 × objective using SPOT software (SPOT, RTke Diagnostic Instruments, Sterling Heights, MI, USA). Nuclei stain blue (i.e., DAPI) and TUNEL positive-nuclei stain green. Corresponding DAPI/TUNEL images were overlaid in photoshop, and a random ∼0.250-mm^2 area selected for counting (i.e., for each of the well, three DAPI images and three TUNEL images were averaged). This procedure was repeated in six separate wells (*n* = 3, control; *n* = 3, injury). The % TUNEL positive nuclei were obtained, and data analyzed using an unpaired *t*-test.

Caspase-3 drug screening assay. An *in vitro* caspase drug screening kit was purchased from PromoKine (Heidelberg, Germany), and used according to the manufacturer's instructions. Briefly, all drugs were dissolved in DMSO and diluted in double-distilled water to desired concentration. The reaction mixture was combined with recombinant active caspase-3 and a DEVD-AFC probe. Active caspase-3 cleaves the DEVD-recognition sequence and releases fluorescent AFC. The amount of AFC detected is a measure of caspase-3 activity. Reactions were prepared in black-walled 96-well plates, incubated at 37 °C, and AFC release measured with an AFC filter (Ex: 405 nM, Em: 495–505 nM) on a GLOMax-Multi

Microplate Reader (Promega). A single data point (value = 15.51462) in the caspase-3 control (no inhibitor) group (data set: mean = 40.60833 and S.D. = 10.67385) was removed from statistical analysis. The value was a significant outlier (*P* < 0.05), as determine by the Grubbs' test.

Western blot analysis. Neurons were grown in six-well plates, treated with experimental compounds for the indicated time/conditions, and harvested for western blot analysis. Extracts were collected in 5-ml tubes, sonicated for 20–30 s, spun at 4 °C/16000 g/10 mins, and stored at − 80 °C until use. Protein concentration was measured using the BCA assay (Pierce, Rockford, IL, USA). 10–20 μg of sample protein was loaded per well of a 7.5% SDS precast gel (Bio-Rad, Hercules, CA, USA), and run for 30 min–1 h at 200 V. Kaleidoscope protein standards (Bio-Rad) were run parallel to neuron extracts. Proteins were then transferred to PDVF membranes (run at 100 V/4 °C/1.5 h). PDVF membranes were washed once in tris-buffered saline (TBS) and blocked for 1 h in tris-buffered saline/Tween-20 with 7.5% non-fat milk (TBS-T/milk). Blots were incubated overnight at 4 °C with primary antibodies in TBS-T/milk. *Cell Signaling Technology* (Danvers, MA, USA): phospho-AKT473, AKT total, phospho-ERK1/2, ERK total, cleavage caspase-3, poly ADP ribose polymerase total, α-tubulin. *Santa Cruz Antibodies* (Santa Cruz, CA, USA): NF-κB p50 subunit, NF-κB p65 subunit, and β actin. *Calbiochem*/EMD Millipore Corporation (Billerica, MA, USA): 4-HNE antibody. Blots were washed three times (5 mins each) with TBS, and incubated with secondary antibodies for 2 h. *Invitrogen*: goat anti-rabbit or goat anti-mouse. Blots were washed three times (5 mins each) with TBS, and incubated for 1 min in HRP detection solution (Amersham/GE Healthcare, Pittsburgh, PA, USA). Films were exposed to blots and developed (SRX-101A, Konica Minolta Medical & Graphic Inc.). Re-probed blots (e.g., β actin, AKT total, ERK total) were stripped in western blot stripping buffer (Fischer Scientific, Pittsburgh, PA, USA) for 10 mins, washed once with TBS, re-blocked in TBS-T/milk for 1 h, and incubated overnight with new primary antibody. Films were scanned (EPSON GT 20000), and densitometry performed using UN-SCAN-IT software (Silk Scientific, Orem, UT, USA).

Statistics. Data were graphed using GraphPad Prism (GraphPad Software Inc., La Jolla, CA, USA) GraphPad statistical software was used to perform unpaired *t*-test analysis. NCSS statistical software (NCSS, Kaysville, UT, USA) was used for one-way-analysisof-variance. If a data set had large unequal variances, the data were first transformed to log base 10 values, and the transformed values analyzed using NCSS. Data are significant at *P* < 0.05.

Conflict of Interest

The authors disclose that a provisional patent has been filed through the University of Pittsburgh's Office of Technology and Management on this work.

1. Greidanus J, Willemse PH, Uges DR, Oremus ET, De Langen ZJ, De Vries EG. Continuous infusion of low-dose doxorubicin, epirubicin and mitoxantrone in cancer chemotherapy: a review. *Pharm Weekbl Sci* 1988; **10**: 237–245.
2. Patterson LH. Bioreductively activated antitumor N-oxides: the case of AQ4N, a unique approach to hypoxia-activated cancer chemotherapy. *Drug Metab Rev* 2002; **34**: 581–592.
3. Wald A. Is chronic use of stimulant laxatives harmful to the colon? *J Clin Gastroenterol* 2003; **36**: 386–389.
4. Kumar A, Katiyar SB, Agarwal A, Chauhan PM. Perspective in antimalarial chemotherapy. *Curr Med Chem* 2003; **10**: 1137–1150.
5. Winter RW, Cornell KA, Johnson LL, Ignatushchenko M, Hinrichs DJ, Riscoe MK. Potentiation of the antimalarial agent rufigallol. *Antimicrob Agents Chemother* 1996; **40**: 1408–1411.
6. Martinelli V, Radaelli M, Straffi L, Rodegher M, Comi G. Mitoxantrone: benefits and risks in multiple sclerosis patients. *Neurol Sci* 2009; **30**(Suppl 2): S167–S170.
7. Kingwell E, Koch M, Leung B, Isserow S, Geddes J, Rieckmann P *et al.* Cardiotoxicity and other adverse events associated with mitoxantrone treatment for MS. *Neurology* 2010; **74**: 1822–1826.

8. Pickhardt M, Gazova Z, von Bergen M, Khlistunova I, Wang Y, Hascher A et al. Anthraquinones inhibit tau aggregation and dissolve Alzheimer's paired helical filaments in vitro and in cells. J Biol Chem 2005; **280**: 3628–3635.

9. Liu T, Jin H, Sun QR, Xu JH, Hu HT. Neuroprotective effects of emodin in rat cortical neurons against beta-amyloid-induced neurotoxicity. Brain Res 2010; **1347**: 149–160.

10. Liu T, Hu HT, Sun QR. [Neuroprotective effects of emodin on primary rat cortical neurons apoptosis induced by hydrogen peroxide]. Zhong Yao Cai 2010; **33**: 1116–1119.

11. Wang C, Zhang D, Ma H, Liu J. Neuroprotective effects of emodin-8-O-beta-D-glucoside in vivo and in vitro. Eur J Pharmacol 2007; **577**: 58–63.

12. Convertino M, Pellarin R, Catto M, Carotti A, Caflisch A. 9,10-Anthraquinone hinders beta-aggregation: how does a small molecule interfere with A beta-peptide amyloid fibrillation? Protein Sci 2009; **18**: 792–800.

13. Colombo R, Carotti A, Catto M, Racchi M, Lanni C, Verga L et al. CE can identify small molecules that selectively target soluble oligomers of amyloid beta protein and display antifibrillogenic activity. Electrophoresis 2009; **30**: 1418–1429.

14. Kwon YS, Koh JY, Song DK, Kim HC, Kwon MS, Choi YS et al. Danthron inhibits the neurotoxicity induced by various compounds causing oxidative damages including beta-amyloid (25-35) in primary cortical cultures. Biol Pharm Bull 2004; **27**: 723–726.

15. Magrane J, Rosen KM, Smith RC, Walsh K, Gouras GK, Querfurth HW. Intraneuronal beta-amyloid expression downregulates the Akt survival pathway and blunts the stress response. J Neurosci 2005; **25**: 10960–10969.

16. Yin KJ, Lee JM, Chen H, Xu J, Hsu CY. Abeta25-35 alters Akt activity, resulting in Bad translocation and mitochondrial dysfunction in cerebrovascular endothelial cells. J Cereb Blood Flow Metab 2005; **25**: 1445–1455.

17. Frew T, Powis G, Berggren M, Abraham RT, Ashendel CL, Zalkow LH et al. A multiwell assay for inhibitors of phosphatidylinositol-3-kinase and the identification of natural product inhibitors. Anticancer Res 1994; **14**: 2425–2428.

18. Olsen BB, Bjorling-Poulsen M, Guerra B. Emodin negatively affects the phosphoinositide 3-kinase/AKT signalling pathway: a study on its mechanism of action. Int J Biochem Cell Biol 2007; **39**: 227–237.

19. Su YT, Chang HL, Shyue SK, Hsu SL. Emodin induces apoptosis in human lung adenocarcinoma cells through a reactive oxygen species-dependent mitochondrial signaling pathway. Biochem Pharmacol 2005; **70**: 229–241.

20. Lai JM, Chang JT, Wen CL, Hsu SL. Emodin induces a reactive oxygen species-dependent and ATM-p53-Bax mediated cytotoxicity in lung cancer cells. Eur J Pharmacol 2009; **623**: 1–9.

21. Perry SW, Norman JP, Litzburg A, Gelbard HA. Antioxidants are required during the early critical period, but not later, for neuronal survival. J Neurosci Res 2004; **78**: 485–492.

22. Vincent AM, Mobley BC, Hiller A, Feldman EL. IGF-I prevents glutamate-induced motor neuron programmed cell death. Neurobiol Dis 2004; **16**: 407–416.

23. Hung KS, Tsai SH, Lee TC, Lin JW, Chang CK, Chiu WT. Gene transfer of insulin-like growth factor-I providing neuroprotection after spinal cord injury in rats. J Neurosurg Spine 2007; **6**: 35–46.

24. Heck S, Lezoualc'h F, Engert S, Behl C. Insulin-like growth factor-1-mediated neuroprotection against oxidative stress is associated with activation of nuclear factor kappaB. J Biol Chem 1999; **274**: 9828–9835.

25. Schmitt TL, Klein H, Droge W. Hydrogen peroxide inhibits activity of the IGF-1 receptor kinase. Redox Rep 2006; **11**: 105–109.

26. Davila D, Torres-Aleman I. Neuronal death by oxidative stress involves activation of FOXO3 through a two-arm pathway that activates stress kinases and attenuates insulin-like growth factor I signaling. Mol Biol Cell 2008; **19**: 2014–2025.

27. Zhong J, Lee WH. Hydrogen peroxide attenuates insulin-like growth factor-1 neuroprotective effect, prevented by minocycline. Neurochem Int 2007; **51**: 398–404.

28. Koh JY, Wie MB, Gwag BJ, Sensi SL, Canzoniero LM, Demaro J et al. Staurosporine-induced neuronal apoptosis. Exp Neurol 1995; **135**: 153–159.

29. Krohn AJ, Preis E, Prehn JH. Staurosporine-induced apoptosis of cultured rat hippocampal neurons involves caspase-1-like proteases as upstream initiators and increased production of superoxide as a main downstream effector. J Neurosci 1998; **18**: 8186–8197.

30. Pike BR, Zhao X, Newcomb JK, Wang KK, Posmantur RM, Hayes RL. Temporal relationships between de novo protein synthesis, calpain and caspase 3-like protease activation, and DNA fragmentation during apoptosis in septo-hippocampal cultures. J Neurosci Res 1998; **52**: 505–520.

31. Deshmukh M, Johnson EM Jr. Staurosporine-induced neuronal death: multiple mechanisms and methodological implications. Cell Death Differ 2000; **7**: 250–261.

32. Kang KH, Lee KH, Kim MY, Choi KH. Caspase-3-mediated cleavage of the NF-kappa B subunit p65 at the NH2 terminus potentiates naphthoquinone analog-induced apoptosis. J Biol Chem 2001; **276**: 24638–24644.

33. Fischer U, Janicke RU, Schulze-Osthoff K. Many cuts to ruin: a comprehensive update of caspase substrates. Cell Death Differ 2003; **10**: 76–100.

34. Leitao JM, Esteves da Silva JC. Firefly luciferase inhibition. Pharm Weekbl Sci 2010; **101**: 1–8.

35. Thorne N, Auld DS, Inglese J. Apparent activity in high-throughput screening: origins of compound-dependent assay interference. Curr Opin Chem Biol 2010; **14**: 315–324.

36. Maddigapu PR, Bedini A, Minero C, Maurino V, Vione D, Brigante M et al. The pH-dependent photochemistry of anthraquinone-2-sulfonate. Photochem Photobiol Sci 2010; **9**: 323–330.

37. Jenkins LW, Peters GW, Dixon CE, Zhang X, Clark RS, Skinner JC et al. Conventional and functional proteomics using large format two-dimensional gel electrophoresis 24 hours after controlled cortical impact in postnatal day 17 rats. J Neurotrauma 2002; **19**: 715–740.

38. Carloni S, Girelli S, Buonocore G, Longini M, Balduini W. Simvastatin acutely reduces ischemic brain damage in the immature rat via Akt and CREB activation. Exp Neurol 2009; **220**: 82–89.

39. Dhandapani KM, Wade FM, Wakade C, Mahesh VB, Brann DW. Neuroprotection by stem cell factor in rat cortical neurons involves AKT and NFkappaB. J Neurochem 2005; **95**: 9–19.

40. Zhang X, Chen Y, Ikonomovic MD, Nathaniel PD, Kochanek PM, Marion DW et al. Increased phosphorylation of protein kinase B and related substrates after traumatic brain injury in humans and rats. J Cereb Blood Flow Metab 2006; **26**: 915–926.

41. Zhao H, Shimohata T, Wang JQ, Sun G, Schaal DW, Sapolsky RM et al. Akt contributes to neuroprotection by hypothermia against cerebral ischemia in rats. J Neurosci 2005; **25**: 9794–9806.

42. Shein NA, Tsenter J, Alexandrovich AG, Horowitz M, Shohami E. Akt phosphorylation is required for heat acclimation-induced neuroprotection. J Neurochem 2007; **103**: 1523–1529.

43. Zhan L, Wang T, Li W, Xu ZC, Sun W, Xu E. Activation of Akt/FoxO signaling pathway contributes to induction of neuroprotection against transient global cerebral ischemia by hypoxic pre-conditioning in adult rats. J Neurochem 2010; **114**: 897–908.

44. Bolton JL, Trush MA, Penning TM, Dryhurst G, Monks TJ. Role of quinones in toxicology. Chem Res Toxicol 2000; **13**: 135–160.

45. Ravati A, Ahlemeyer B, Becker A, Krieglstein J. Preconditioning-induced neuroprotection is mediated by reactive oxygen species. Brain Res 2000; **866**: 23–32.

46. Zhou X, Wang L, Wang M, Xu L, Yu L, Fang T et al. Emodin-induced microglial apoptosis is associated with TRB3 induction. Immunopharmacol Immunotoxicol 2011; **33**: 594–602.

47. Lee YJ, Shacter E. Hydrogen peroxide inhibits activation, not activity, of cellular caspase-3 in vivo. Free Radic Biol Med 2000; **29**: 684–692.

48. Hampton MB, Orrenius S. Dual regulation of caspase activity by hydrogen peroxide: implications for apoptosis. FEBS Lett 1997; **414**: 552–556.

49. Moore JD, Rothwell NJ, Gibson RM. Involvement of caspases and calpains in cerebrocortical neuronal cell death is stimulus-dependent. Br J Pharmacol 2002; **135**: 1069–1077.

50. Goswami R, Kilkus J, Dawson SA, Dawson G. Overexpression of Akt (protein kinase B) confers protection against apoptosis and prevents formation of ceramide in response to pro-apoptotic stimuli. J Neurosci Res 1999; **57**: 884–893.

51. Holton H. Soda Additive Softwood Pulping - Major New Process. Pulp Pap-Canada 1977; **78**: 19–24.

52. Ziderman II, Belayche J. Effect of anthraquinones on endwise degradation of hydrocellulose in relation to alkaline pulping. Carbohyd Polym 1986; **6**: 109–119.

53. Bien H-S, Stawitz J, Wunderlich K. Anthraquinone dyes and intermediates. Ullmann's Encyclopedia of Industrial Chemistry. 2000.

54. Leskovac V, Trivic S, Peggins JO. Primary toxic effects of anthraquinone-2-sulfonic acid in rat liver microsomes. Toxicol Lett 1995; **78**: 107–110.

55. Adams GE, Clarke ED, Jacobs RS, Stratford IJ, Wallace RG, Wardman P et al. Mammalian cell toxicity of nitro compounds: dependence upon reduction potential. Biochem Biophys Res Commun 1976; **72**: 824–829.

56. Bayol-Denizot C, Daval JL, Netter P, Minn A. Xenobiotic-mediated production of superoxide by primary cultures of rat cerebral endothelial cells, astrocytes, and neurones. Biochim Biophys Acta 2000; **1497**: 115–126.

57. Winterbourn CC. Cytochrome c reduction by semiquinone radicals can be indirectly inhibited by superoxide dismutase. Arch Biochem Biophys 1981; **209**: 159–167.

58. Fulbright JM, Huh W, Anderson P, Chandra J. Can anthracycline therapy for pediatric malignancies be less cardiotoxic? Curr Oncol Rep 2010; **12**: 411–419.

59. Vile GF, Winterbourn CC. Microsomal reduction of low-molecular-weight Fe3 + chelates and ferritin: enhancement by adriamycin, paraquat, menadione, and anthraquinone 2-sulfonate and inhibition by oxygen. Arch Biochem Biophys 1988; **267**: 606–613.

60. Jackson TC, Verrier JD, Semple-Rowland S, Kumar A, Foster TC. PHLPP1 splice variants differentially regulate Akt and PKCalpha signaling in hippocampal neurons: characterization of PHLPP proteins in the adult hippocampus. J Neurochem 2010; **115**: 941–955.

Supplementary Information accompanies the paper on Cell Death and Disease website (http://www.nature.com/cddis)